Journal of Metals, Materials and Minerals, 34(2), 1957, 2024

Green synthesis of carbon dots from mangosteen peel for fluorescent cancer cells

Supaluck AMLOY[1,2,*], Tanachporn LUKPRANG[1], Monthon LERTWORAPREECHA[3], and Pakorn PREECHABURANA[1,2]

[1] Department of Physics, Faculty of Science and Technology, Thammasat University, Pathum Thani 12120, Thailand.
[2] Thammasat University Research Unit in Innovation of Optical Devices and Nanomaterials for Chemical and Biological Sensing, Thammasat University, Pathum Thani 12120, Thailand.
[3] Microbial Technology for Agriculture, Food and Environment Research Center, Faculty of Science, Thaksin University, Phatthalung, 93210, Thailand.

***Corresponding author e-mail**: supalucka@tu.ac.th

Received date:
5 February 2024
Revised date
20 March 2024
Accepted date:
24 April 2024

Keywords:
Carbon dots;
Mangosteen peel;
Fluorescence;
Caco-2 cells

Abstract

Recently, carbon dots (CDs) have received significant attention owing to their outstanding optical properties, good solubility, and low toxicity. In this research, CDs were synthesized by a hydrothermal method based on an environmentally friendly and straightforward strategy, using only mangosteen peel and deionized water. The synthesized CDs had an average size of 3.09 ± 0.38 nm. The absorbance spectrum peak for the CDs was seen at 282 nm, and the central wavelength of fluorescence emission was observed at 433 nm under an excitation wavelength of 355 nm. An aqueous solution of CDs exhibited bright green fluorescence when observed with the naked eye under UV irradiation. Both Fourier transform infrared and X-ray photoelectron spectroscope measurements were taken to determine the elemental compositions of the organic substance functional groups on the surface of the CD, such as hydroxyl, carboxyl, and carbonyl groups. These functional groups originate the different emission centers leading to multicolor fluorescent emissions. Furthermore, the synthesized CDs were found to have good biocompatibility with organic and biological materials. The remarkable properties of CDs, including their nanoscale dimensions, strong multicolor fluorescent emissions, non-toxicity, and excellent cell compatibility, could effectively permeate the cell membrane, cytoplasm, and nucleus and provide fluorescence emission. This suggests a significant potential for CDs in fluorescent cell staining applications. Finally, the CDs were used as a fluorescent dye for human colon cancer cells, as they exhibited excellent fluorescence for cell staining.

1. Introduction

The technique of fluorescence bioimaging is a crucial tool for clinical diagnosis and therapy assessment, and a continuous development process of fluorescent agent probes is ongoing. Colloidal quantum dots (CQDs) are in widespread use as fluorescent probes, both as labels and as contrast agents in biological staining. The superior advantages of CQDs over conventional fluorophores are their sharp emissions, symmetric spectra, and photostability [1]. However, CQDs are most frequently employed in cell dyeing applications involving heavy metals such as CdSe, CdS, CdTe, and CdZnS. However, uncoated CQD materials have the potential to generate cadmium ions, leading to toxicity in cells, and it is therefore essential to apply biocompatible coating substances to cover their surfaces. For instance, a CdSe and CdS nanocrystal enclosed in a silica shell in an aqueous buffer can emit green (2-nm core) and red (4-nm core) fluorescence [2]. Poly (N-isopropylacrylamide)-encapsulated CdTe nanospheres exhibit good colloidal stability and strong green luminescence [3], and liposomal encapsulated CdSe/CdZnS emit red light [4]. Hence, the use of CQDs for bioimaging applications has been restricted due to complications related to the biocompatibility of nanomaterials and the possibility of environmental risk. These drawbacks can be overcome by a new type of fluorescent nanomaterial with good biocompatibility and environmental friendliness.

In recent years, fluorescent carbon dots (CDs) have been considered ideal as fluorescent bioimaging agent probes due to their multi-color fluorescence, tunable emissions, photostability, resistance to photo-bleaching, ease of functionalization, excellent biocompatibility, good solubility in aqueous and organic solvents, low cost, simplicity of production, and low toxicity and environmental risk [5-7]. The CDs exhibited an extremely high quantum yield of 48% [8] and demonstrated tunable emissions, including red, green, and blue emissions [7]. Furthermore, the biocompatibility and bioimaging potential of fruit-based CDs were demonstrated. In vivo, toxicity assessment was performed using zebrafish embryos. Both in vitro and in vivo experiments revealed that the synthesized CDs exhibited toxicity only at concentrations exceeding 1.5 mg·mL^{-1} [5]. A simple functionalized CD by chemical modification with ethylenediamine to form amide bonds. This resulted

in a notable ability to selectively stain nucleoli in breast cancer cell lines (MCF-7), demonstrating remarkable precision cellular targeting [9]. An emerging area of research involves cell staining with CDs, which can be synthesized from organic or inorganic precursors. Organic substances serve as the principal reactants, including graphite rods [10] and mixture of glucose, 1,2-ethylenediamine, and phosphoric [11], P-phenylenediamine [12], glycerol [13], and o-phenylenediamine [14]. Additional organic precursors include apple juice [15], unripe peaches [16], saffron [17], mangosteen pulp [18], ayurvedic plant leaves [19], mango peel [20], prunus cerasifera fruits [21], and cherry blossom flowers [22]. CDs have found applications not only in fluorescent biological imaging but also in various areas such as biosensing [23], targeted drug delivery [24], photocatalysis [25], fluorescent inks [26], solar cells [27], and light-emitting devices [28]. This wide range of applications has given rise to a growing number of research areas related to CDs. However, CDs, being fluorescent nanoparticles, show a growing trend to be used as nanocarriers and bioimaging agents for delivering drugs or specific molecules to cancer cells. This emerging may provide a novel tool for both cancer prognosis and treatment [29].

The green synthesis of CDs extracted from a variety of organic materials is also interesting for bioimaging applications. In this article, we report the strong and tunable fluorescent emission of CDs fabricated using a green synthesis method without a chemical reactant and using mangosteen peel as a carbon precursor. As well as mangosteen is widely cultivated in Thailand and serves as an economic export fruit. Consequently, a large amount of mangosteen peel is generated as waste material. Therefore, synthesizing waste materials like mangosteen peel into carbon dots is a significant advantage. Furthermore, carbon dots can be used as fluorescent strain cells and for various future nano-technology applications. Nevertheless, there are few research reports on the utilization of CDs for cell straining with strong emissions that could span across green, blue, and red [17,20]. Furthermore, the novelty of this work lies in the first synthesis of CDs from mangosteen peel using the hydrothermal method. Although there is one report of synthesizing CDs from the same carbon source, mangosteen peel, it utilized a different method which was pyrolysis [30]. Moreover, a report has utilized CDs for staining human colon cancer cells (Caco-2 cells) demonstrating only two colors of emission: green and red [31]. However, the synthesized CDs in this work have the potential for use in staining Caco-2 cells via strong multicolor fluorescent emissions over the spectral spanning green, blue, and red.

2. Experiments

2.1 Materials and instrumentation

Mangosteens (*Garcinia mangostana* L.) well thrive in tropical weather countries, particularly in the eastern and southern provinces of Thailand. There is only one species of mangosteen grown in Thailand. In this research, mangosteens were bought from a fruit market (Krabi, Thailand). The selected mangosteens were the size of 4 cm to 6 cm in diameter, round, fresh, fully mature, reddish-purple in color, and smooth peel without any yellow sap. All the chemicals used in this research were analytical grade, and were used without any further purification. Quinine sulphate (99%, standard fluorescence quantum yield) and sulfuric acid (H_2SO_4) were purchased from Sigma-Aldrich. Dulbecco's Modified Eagle's Medium (DMEM) containing 10% fetal bovine serum (FBS), penicillin 1,000 units·mL^{-1}, streptomycin 1,000 µg·mL^{-1}, amphotericin B 2,500 µg·mL^{-1}, dimethyl sulfoxide (DMSO), and phosphate-buffered saline (PBS) were obtained from Cytiva. The 96-well plates and 3-(4,5-dimethylthiazol-2-yl)-2,5-diphenyltetrazolium bromide (MTT) were purchased from Thermo Scientific.

Transmission electron microscope (TEM) images were acquired using a JEM-2100 electron microscope (JEOL, Japan). The zeta potential of the CDs was measured with a Partica LA-950V2 (Horiba). X-ray diffraction (XRD) analysis was carried out using a D2 PHASER X-ray diffractometer (Bruker). The FTIR spectra were measured with a Nicolet iS50 instrument (Thermo Scientific). XPS measurements were made using an AXIS Ultra DLD spectrometer (Kratos Analytical Ltd., Manchester, UK). The UV–visible absorption and fluorescence spectra of the CDs were recorded using a Duetta (Horiba) spectrophotometer (Tokyo, Japan). The fluorescence lifetime was recorded on a FluoroMax ®Plus spectrofluorometer (Horiba), and fluorescence microscopic cell imaging was carried out using a BX53 fluorescence microscope (Olympus, Japan). The optical density (OD) of each well solution was measured with an AsysUVM340 microplate reader (Biochrom, UK).

2.2 Synthesis of CDs

CDs were prepared by the hydrothermal method, using mangosteen peel and deionized (DI) water with no chemical solvent. Mangosteen peel (50 g) was chopped into small pieces and mixed with 350 mL DI water, and then ground with a blender into a liquid. The resulting liquid was filtered using Whatman filter paper 11 µm to remove the residue. The mixture was transferred into a Teflon-lines stainless steel autoclave and heated at 200°C for 3 h, and then left to cool down to the ambient temperature. The resulting dark brown solution was filtered with 0.45 µm and 0.22 µm microfiltration membranes to remove large particles. The CD solution was stored at 4°C for further characterization and cell staining. Moreover, the synthesis of CDs by this protocol was a repeatable process and stability which was confirmed through continuous measurement of the optical properties over one month.

2.3 Fluorescence quantum yield measurements

The fluorescence quantum yield of CDs (ϕ_{CDs}) was determined using quinine sulfate in 0.1 M H_2SO_4 solution using as a reference quantum yield (ϕ_{ref} = 0.54) and calculated by following equation

$$\phi_{CDs} = \phi_{ref} \times \left(\frac{K_{CDs}}{K_{ref}}\right) \times \left(\frac{\eta_{CDs}}{\eta_{ref}}\right)^2 \quad (1)$$

where K_{CDs} and K_{ref} represent the slopes between the integrated fluorescence emission intensity and UV-vis absorbance of CDs and quinine sulfate solution, respectively. η_{CDs} and η_{ref} refer to the refractive index of the solvent used.

2.4 Cell culture and CD staining

Caco-2 cells were cultured in 150 µL of DMEM medium supplemented with 10% fetal bovine serum at 37°C and incubated in a 5% CO_2 atmosphere for 48 h. Caco-2 cells were seeded in eight-well chamber slides at a density of 5×10^4 cells/well. Then, 150 µL of the CD solution was added to each well and the slides were incubated for 24 h. Following this, the cells were washed three times using a PBS buffer to remove residual CDs. Finally, fluorescence imaging of the cells was performed using a fluorescence microscope with different excitation wavelengths of 403 nm (DAPI), 498 nm (FITC), and 570 nm (TXRED).

3. Results and discussion

3.1 Characterization of the CDs

TEM imaging was carried out to estimate the size and morphology of the synthesized CDs by using the open-source Image J program. The appearance of the CDs was well dispersion and spherical, with an average size of 3.09 ± 0.38 nm (Figure 1(a-b)). In addition, the zeta potential of the CDs was measured as –26.9 mV (Figure 1(c)), which represents the formation of good dispersion due to sufficient mutual repulsion. The dispersion results consistently agreed with the TEM images. Thus, the good dispersion of CDs makes them suitable for use as a high-performance dyeing cell solution [32,33]. To analyze the crystal plane, the carbon dot solution was baked at 100 degrees without any compression. The crystal planes of carbon dot particle agglomeration were measured by an X-ray diffractometer. Sharp XRD peaks were observed at 28.4°, 40.7°, 50.4°, and 58.9°, corresponding to the crystal planes (002), (100), (102), and (103), respectively, indicating that the CDs are crystalline. The first three of these planes are associated with graphite (sp^2), while the last corresponds to diamond (sp^3). The calculated d-spacings for (002), (100), (102), and (103) are 0.31 nm, 0.22 nm, 0.18 nm, and 0.16 nm, respectively, indicating a resemblance to graphite [1]. These d-spacing results are consistent with reference 34 which was characterized by using both XRD and high-resolution transmission electron microscope (HRTEM) [34].

3.2 Surface functional groups

The presence of the surface functional group was validated by FTIR and XPS analysis. A comparison of the FTIR spectra for CDs and mangosteen peel extract (see Figure 2(a) and Table 1) revealed that the functional groups, such as the O-H stretching vibration (hydroxyl function groups, peaks between 3200 cm^{-1} and 3500 cm^{-1}), C–H (graphitic structure, peak between 2775 cm^{-1} and 3000 cm^{-1}), C=C (peak between 1445 cm^{-1} and 1600 cm^{-1}), –OH/(C–OH) (peak between 1330 cm^{-1} and 1445 cm^{-1}), C–O (acid/C–OH) (peak between 1150 cm^{-1} and 1330 cm^{-1}), and C–O–C (peak between 900 $cm^{-1}$and 1150 cm^{-1}) of the CDs were twice as strong as those of mangosteen peel juice. It was interesting to note that C=O bonding (peak between 1600 cm^{-1} and 1700 cm^{-1}) was found to be almost negligible in the CDs.

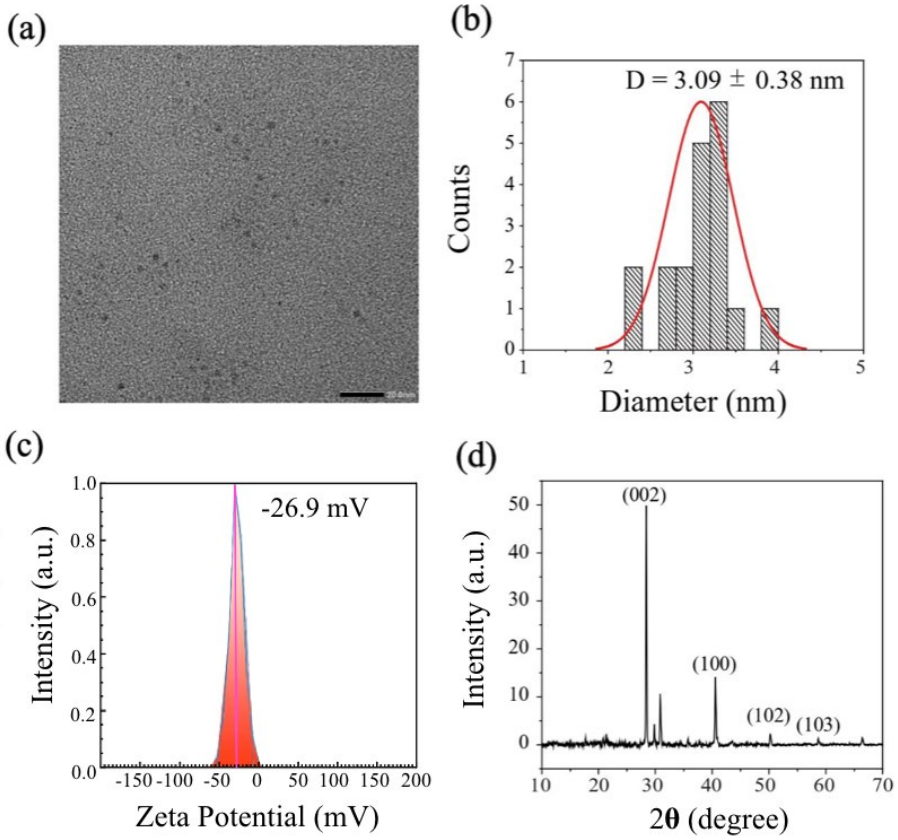

Figure 1. (a) Transmission electron microscopy images of CDs, (b) their size distribution histograms, (c) zeta potential diagram for CDs, and (d) X-ray diffraction pattern for CDs.

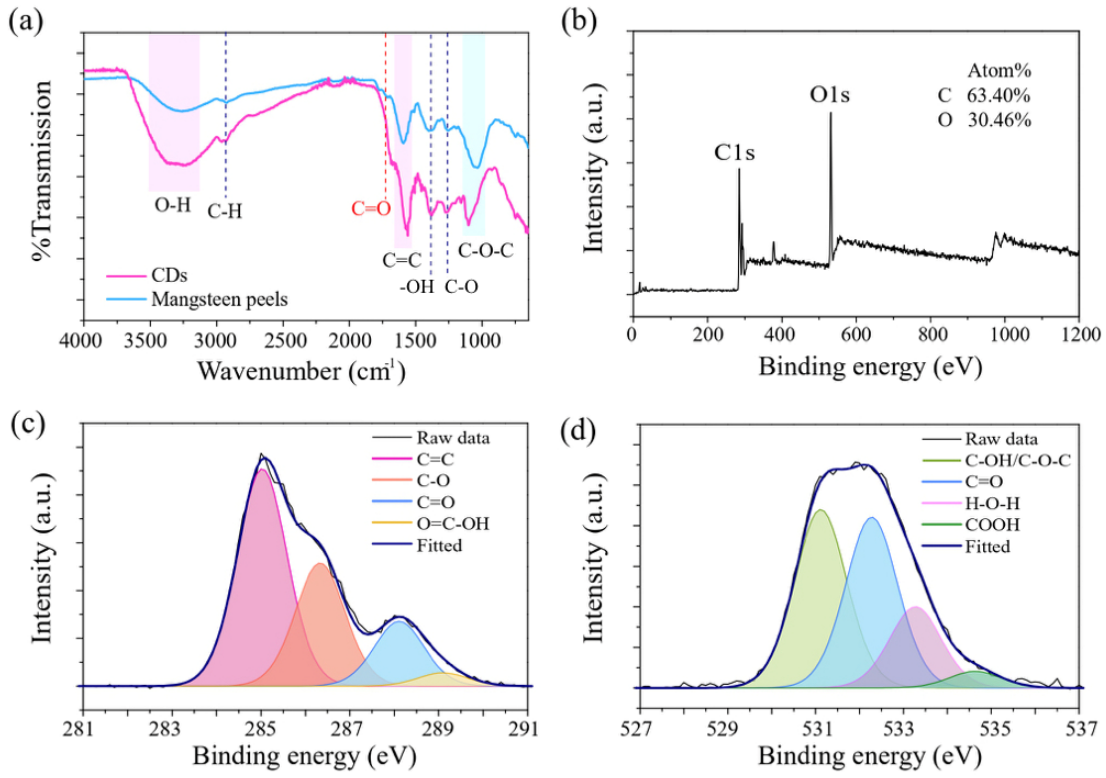

Figure 2. (a) Fourier-transform infrared spectra for CDs and mangosteen peel juice; (b) X-ray photoelectron spectroscopy spectrum for CDs; high-resolution XPS spectra for (c) C1s and (d) O1s.

Table 1. Peak areas for FTIR spectra of mangosteen peel extract and CDs.

Wavenumber (cm^{-1})	Functional groups	Peak area for mangosteen peel extract		Peak area for CDs	
		Wavenumber (cm^{-1})	Intensity (a.u.)	Wavenumber (cm^{-1})	Intensity (a.u.)
900 - 1150	(C–O–C) ether	1043.96	33.85	1088.70	51.37
1150 - 1330	(C–O) (Acid/C–OH)	1249.03	21.29	1258.35	49.13
1330 - 1445	(O–H/C-OH)	1392.57	21.36	1362.74	49.16
1445 - 1600	(C=C) Aromatic ring	1593.91	25.70	1567.81	54.54
1600 - 1700	(C=O) carbonyl group	1718.72	10.09	-	-
2775 - 3000	(C–H) Graphitic structure	2924.96	11.93	2973.43	24.86
3200 - 3500	(O–H) hydroxyl	3266.11	14.83	3253.06	32.89

The surface functional groups of the CDs were confirmed by the XPS results. A survey XPS spectrum (Figure 2(b)) also verified the dominant elements of C1s and O1s, at energies of 285 eV and 532 eV, respectively, and the atomic concentrations of C and O elements were 63.40% and 30.46%, respectively. A high-resolution analysis of the C1s spectrum (Figure 2(c)) showed four peaks at 285.0 eV, 286.3 eV, 288.1 eV, and 289.1 eV, corresponding to C=C, C–O, C=O, and O=C–OH bonds. The high resolution of the O1s spectrum (Figure 2(d)) confirmed the presence of C–OH/C–OC, C=O, H–OH, and COOH, corresponding to energies of 531.1, 532.3, 533.3, and 534.6 eV, respectively. The FTIR and XPS results confirmed that the synthesized CDs contained graphitic carbon (C=C, CD core atoms), which was attached to functional groups such as hydroxyl, carboxyl, and carbonyl. These surface functional groups represent the high solubility in water and organic media, and the existence of a large fraction of defects mainly resulted from surface oxidation originating from the fluorescent emission of CDs [35].

3.3 Optical properties

The optical characteristics of CDs were studied based on the UV–visible absorption and fluorescence spectra. The absorbance of the CDs shows a dominant peak at 282 nm, which was attributed to the π-π* transition of C=C bonds (carbon core). The mangosteen peel extract shows a shoulder peak at 282 nm (Figure 3(a)). Moreover, no fluorescent emission is observed for mangosteen peel extract (with an excitation wavelength of 270 nm) (inset to Figure 3(a)), while the CDs exhibited strong emission at 295 nm and 430 nm. These results are consistent with those of the FTIR analysis, which showed that the C=C bonds (ring structure of carbon core) of the CDs were twice as strong as those of mangosteen peel extract. It was therefore verified that the mangosteen peel extract was transformed into CDs via the formation of a ring structure.

To study the emission mechanism of CDs, the energy gap of the CDs was determined using a Tauc plot, as shown in Figure 3(b), which

was calculated from the transmission spectra (inset to Figure 3(b)). The energy gap for the CDs was found to be 4.03 eV. Fluorescent emission spectra with a dependent excitation wavelength of 250 nm to 450 nm were measured. Figures 4(a-b) show the redshift in the emission with an increase in the excitation wavelength. There are two optimal maximum emissions at 341 nm and 433 nm for excitation wavelengths of 255 nm and 355 nm, respectively. The CDs consisting of hydroxyl, carboxyl, and carbonyl surface functional groups cause a rearrangement of the emission center, which creates the energy states between the energy gap and can trap excitons, causing a redshift in the emission wavelength, as shown in Figure 4(c). Furthermore, the CDs exhibit a strong fluorescence emission, with a quantum yield of 2% and an emission lifetime of 2.5 ns (Figure 3(c)).

Based on the analysis results, the synthesized carbon dots revealed the feature of a carbon core primarily composed of C=C or C–C bonds. Additionally, the surface functionality was bonded from oxygen and hydrogen. This structural composition gives rise to numerous energy states, allowing the carbon dots to emit high-intensity fluorescence in various emission colors with dependence on excitation wavelengths.

3.4 Cell imaging

The Caco-2 cells were stained with aqueous CDs. It was found that the CDs showed good compatibility with cells, and could be efficiently internalized into the cell membrane, cytoplasm, and nucleus. This was because the CDs were synthesized from organic precursors, without a chemical solvent. The sizes of the synthesized CDs were also at the nanoscale, and they showed good solubility in water or organic substances, resulting in good compatibility with cells. Figure 5 shows bright-field and fluorescent images of Caco-2 cells under excitation wavelengths of 403 nm (DAPI), 498 nm (FITC), and 570 nm (TXRED), with strong fluorescence emission of blue, green, and red light, respectively. The multicolor emission properties of CDs offer great advantages for fluorescence bioimaging applications.

In order to assess the CD cell staining efficiency, the fluorescence intensity, with various excitation wavelengths 403 nm, 498 nm, and 570 nm, was analyzed before and after cell staining. The CDs exhibited strong fluorescence intensity when excited at 403 nm, 570 nm, and 498 nm, respectively (Figure 6(a)). While, the fluorescence microscopy intensities of CD-stained cells from digital images were analyzed using an image processing method based on the red, green, and blue (RGB) color space. The fluorescence intensities in the blue, green, and red channels were considered separately. It was found that the fluorescence cell images had the highest light intensity when excited with wavelengths of 403 nm, followed by excitation wavelengths of 570 and 498 nm (Figure 6(b)). Hence, the fluorescence response of CDs both before and after cell staining proved to be highly efficient and consistent.

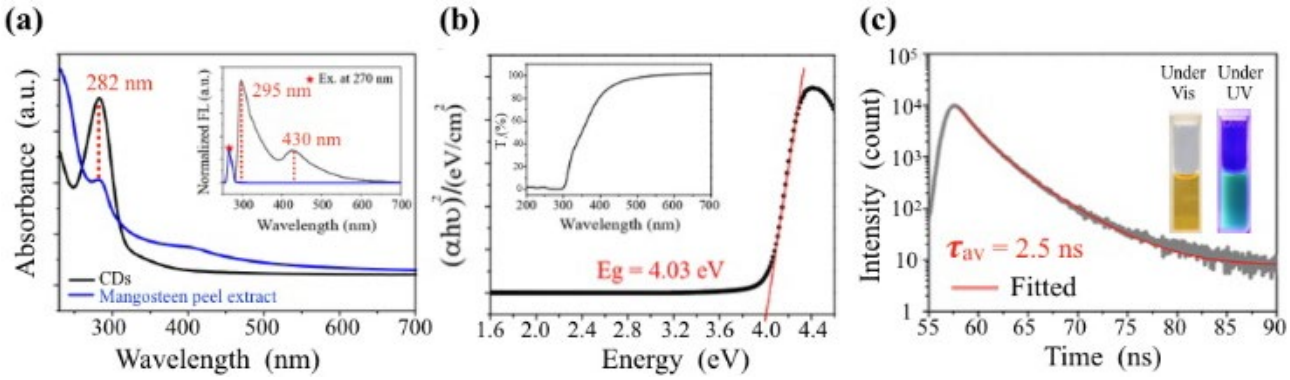

Figure 3. (a) Ultraviolet-visible absorbance spectra; the inset shows the fluorescent emission spectra for CDs (black line) and mangosteen peel extract (blue line) at an excitation wavelength of 270 nm, (b) energy gap fitting with a Tauc plot; the inset shows the transmission spectrum of the CDs, and (c) fluorescence emission lifetime spectrum for excitation wavelength at 370 nm; the inset shows the CD photoemission under visible and UV light.

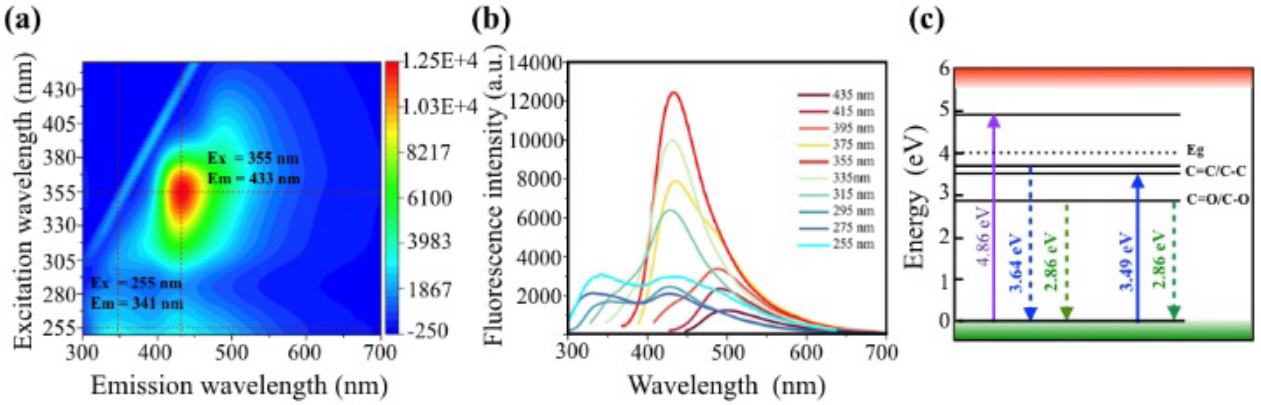

Figure 4. (a) Three-dimension fluorescent emission spectra for CDs with different excitation wavelengths at 250 nm to 450 nm, (b) fluorescent spectra for CDs with different excitation wavelengths at 255 nm to 435 nm, and (c) schematic diagram showing the energy level alignment of CDs corresponding to the optimal excitation energy (solid arrows) for maximum emission (dashed arrows).

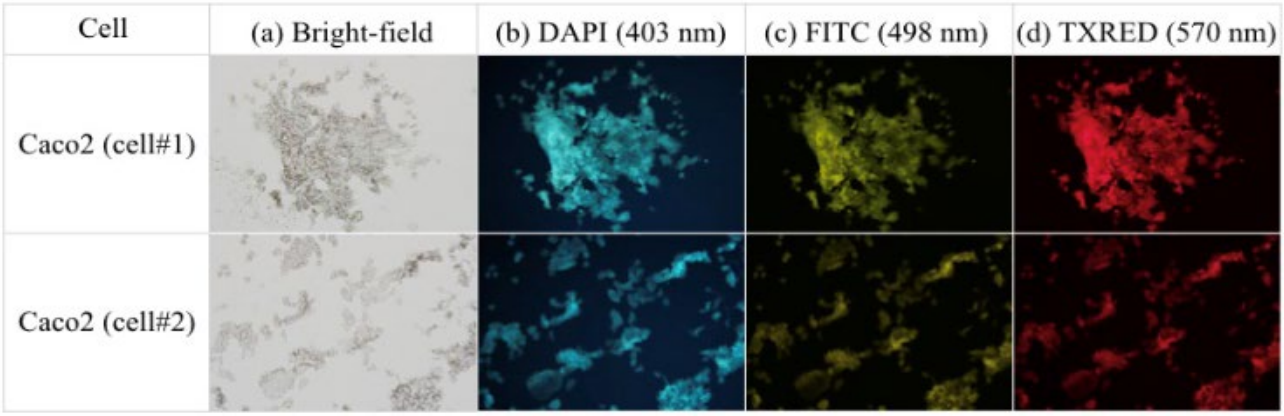

Figure 5. Confocal fluorescence microscopy images of Caco-2 cells in the presence of CDs: (a) bright-field images, images taken at three excitation wavelengths of (b) 403 nm (DAPI), (c) 498 nm (FITC), and (d) 570 nm (TXRED).

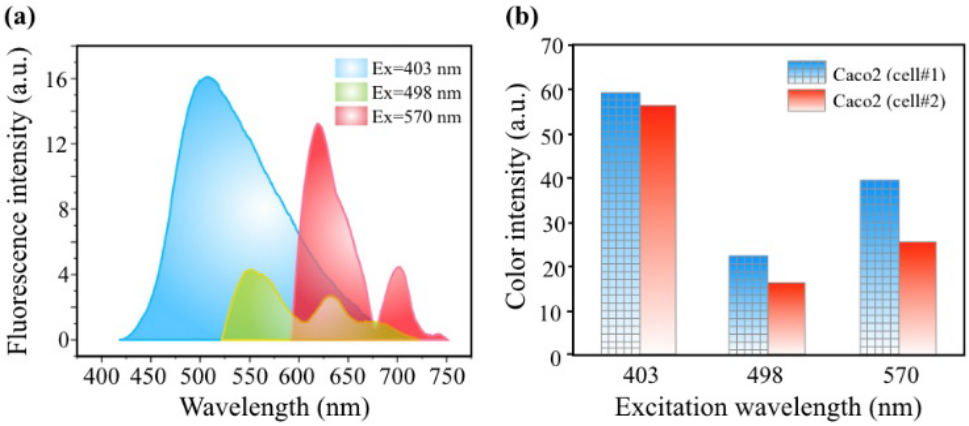

Figure 6. (a) Fluorescent spectra for CDs with three excitation wavelengths at 403 nm, 498 nm, and 570 nm, and (b) graph of the color intensity of confocal fluorescence microscopy images of Caco-2 cells in the presence of CDs, obtained from the images in Figure 5 using the RGB color space.

4. Conclusion

CDs were successfully synthesized by the hydrothermal method using mangosteen peel as a precursor, without the addition of a chemical solution. The CDs had a very small size of 3 nm, and functional surface groups such as hydroxyl, carboxyl, and carbonyl. The CDs exhibited strong multifluorescent emission with different excitation wavelengths from 250 nm to 450 nm, and were able to penetrate the Caco-2 nucleus cells. The highest fluorescent emission from the cell was found for an excitation wavelength of 403 nm. Therefore, the synthesized CDs, distinguished by their nanoscale dimensions, strong multicolor fluorescence emissions, non-toxic, and excellent cell compatibility, demonstrated the ability to penetrate the cell membrane, cytoplasm, and nucleus. These highlights are considered as potential for the utilization of CDs in fluorescent cell staining applications and may provide a novel tool for both cancer prognosis and treatment.

Acknowledgements

This work was supported by grants from Thammasat University Research Fund (Contract No. TUFT 58/2566), Thammasat University Research Unit in Innovation of Optical Devices and Nanomaterials for Chemical and Biological Sensing, and the Thailand Science Research and Innovation Fundamental Fund fiscal year 2022, Thaksin University (Contract No. TSU-65A105000007). The authors would like to thank Department of Physics and Department of Materials Science, Faculty of Science and Technology, Thammasat University for providing access to the optical characterization instruments.

References

[1] M. Bruchez Jr., M. Moronne, P. Gin, S. Weiss, and A. P. Alivisatos, "Semiconductor nanocrystals as fluorescent biological labels," *Science*, vol. 281, pp. 2013-2016, 1998.

[2] N. Thondavada, R. Chokkareddy, N. V. Naidu, and G. G. Redhi, "New generation quantum dots as contrast agent in imaging," *Nanomaterials in Diagnostic Tools and Devices*, Elsevier, pp. 417-437, 2020.

[3] S. G. Mitra, D. R. Diercks, N. C. Mills, D. L. Hynds, and S. Ghosh, "Excellent biocompatibility of semiconductor quantum dots encased in multifunctional poly (N-isopropylacrylamide) nanoreservoirs and nuclear specific labeling of growing neurons," *Applied Physics Letters*, vol. 98, pp. 103702, 2011.

[4] G. Aizik, N.Waiskopf, M. Agbaria, Y. Levi-Kalisman, U. Banin,

and G. Golomb, "Delivery of liposomal quantum dots via monocytes for imaging of inflamed tissue,", *ACS Nano*, vol. 11, pp. 3038-3051, 2017.

[5] C. Dias, N. Vasimalai, M. P. Sárria, I. Pinheiro, V. Vilas-Boas, J. Peixoto, and B. Espiña, "Biocompatibility and bioimaging potential of fruit-based carbon dots," *Nanomaterials*, vol. 9, no. 199, pp. 1-19, 2019.

[6] S. Wahyudi, A. Bahtiar, C. Panatarani, Anas, and Risdiana, "Recent advanced carbon dots derived natural products and aptasensor-based carbon dots for detection of pesticides," *Sensing and Bio-Sensing Research*, vol. 41, pp. 100576, 2023.

[7] J. Liu, R. Li, and B. Yang, "Carbon dots: A new type of carbon-based nanomaterial with wide applications," *ACS Central Science*, vol. 6, pp. 2179-2195, 2020.

[8] N. Alvandi, S. Assariha, N. Esfandiari, and R. Jafari "Off-on sensor based on concentration-dependent multicolor fluorescent carbon dots for detecting pesticides," *Nano-Structures & Nano-Objects*, vol. 26, pp. 100706, 2021.

[9] C. E. S. Barbosa, J. R. Correa, G. A. Medeiros, G. Barreto, K. G. Magalhaes, A. L. Oliveira, J. Spencer, M. O. Rodrigues, and B. A. D. Neto, "Carbon dots (C-dots) from cow manure with impressive subcellular selectivity tuned by simple chemical modification," *Chemistry A European Journal*, vol. 21, pp. 5055-5060, 2015.

[10] W. Kong, J. Liu, R. Liu, H. Li, Y. Liu, H. Huang, K. Li, J. Liu, S.T. Lee, and Z. Kang, "Quantitative and real-time effects of carbon quantum dots on single living HeLa cell mem-brane permeability," *Nanoscale*, vol. 6, pp. 5116, 2014.

[11] X. Gong, Q. Zhang, Y. Gao, S. Shuang, M. M. F. Choi, and C. Dong, "Phosphorus and nitrogen dual-doped hollow carbon dot as a nanocarrier for doxorubicin delivery and biological imaging," *ACS Applied Materials & Interfaces*, vol. 8, pp. 11288-11297, 2016.

[12] Y. Jiao, X. Gong, H. Han, Y. Gao, W. Lu, Y. Liu, M. Xian, S. Shuang, and C. Dong, "Facile synthesis of orange fluorescence carbon dots with excitation independent emission for pH sensing and cellular imaging," *Analytica Chimica Acta*, vol 1042, pp. 125-132, 2018.

[13] J. Yang, G. Gao, X. Zhang, Y. H. Ma, X. Chen, and F. G. Wu, "One-step synthesis of carbon dots with bacterial contact-enhanced fluorescence emission: Fast Gram-type identification and selective Gram-positive bacterial inactivation," *Carbon*, vol. 146, pp. 827-839, 2019.

[14] Q. Zhang, R. Wang, B. Feng, X. Zhong, and K. Ostrikov, "Photoluminescence mechanism of carbon dots: Triggering high-color-purity red fluorescence emission through edge amino protonation," *Nature Communications*, vol. 12, no. 6856, pp. 1-13, 2021.

[15] V. N. Mehta, S. Jha, H. Basu, R.K. Singhal, and S. K. Kailasa, "One-step hydrothermal approach to fabricate carbon dots from apple juice for imaging of mycobacterium and fungal cells," *Sensors Actuators B: Chemical*, vol. 213, pp. 434-443, 2015.

[16] R. Atchudan, T. Edison, and Y.R. Lee, "Nitrogen-doped carbon dots originating from unripe peach for fluorescent bioimaging and electrocatalytic oxygen reduction reaction," *Journal of Colloid and Interface Science*, vol. 482, pp. 8-18, 2016.

[17] A. A. Ensafi, S. S. Hghighat, N. Kazemifard, B. Rezaei, and F. Moradi, "A novel one-step and green synthesis of highly fluorescent carbon dots from saffron for cell imaging and sensing of prilocaine," *Sensor and Actuators B: Chemical*, vol. 253, pp. 451-460, 2017.

[18] R. Yang, X. Guo, L. Jia, Y. Zhang, Z. Zhao, and F. Lonshakov, "Green preparation of carbon dots with mangosteen pulp for the selective detection of Fe^{3+} ions and cell imaging," *Applied Surface Science*, vol. 423, pp. 426-432, 2017.

[19] R. Meena, R. Singh, G. Marappan, G. Kushwaha, N. Gupta, R. Meena, J. P. Gupta, R. R. Agarwal, N. Fahmi, and O. S. Kushwaha, "Fluorescent carbon dots driven from ayurvedic medicinal plants for cancer cell imaging and phototherapy," *Heliyon*, vol. 5, pp. e02483, 2019.

[20] X. Y. Jiao, L. S. Li, S. Qin, Y. Zhang, K. Huang, and L. Xu, "The synthesis of fluorescent carbon dots from mango peel and their multiple applications," *Colloids and Surfaces A: Physico-chemical and Engineering Aspects*, vol. 577, pp. 306-314, 2019.

[21] H. Ma, C. Sun, G. Xue, G. Wu, X. Zhang, X. Han, X. Qi, X. Lv, H. Sun, and J. Zhang, "Facile synthesis of fluorescent carbon dots from Prunus cerasifera fruits for fluorescent ink, Fe^{3+} ion detection and cell imaging," *Spectrochimca Acta A: Molecular Biomolecular Spectroscopy*, vol. 213, pp. 281-287, 2019.

[22] K. Huang, Q. He, R. Sun, L. Fang, H. Song, L. Li, Z. Li, Y. Tian, H. Cui, and J. Zhang, "Preparation and application of carbon dots derived from cherry blossom flowers," *Chemical Physics Letter*, vol. 731, p. 136586, 2019.

[23] C. Ji, Y. Zhou, R. M. Leblanc, and Z. Peng, "Recent developments of carbon dots in biosensing: A review," *ACS Sensors*, vol. 5, pp. 2724-2741, 2020.

[24] A. A. Ridha, P. Pakravan, A. H. Azandaryani, and H. Zhaleh, "Carbon dots: The smallest photoresponsive structure of carbon in advanced drug targeting," *Journal of Drug Delivery Science and Technology*, vol. 55, pp. 101408, 2019.

[25] K. A. S. Fernando, S. P. Sahu, Y. Liu, W. K. Lewis, E. Guliants, A. Jafariyan, P. Wang, C. E. Bunker, and Y. P. Sun, "Carbon quantum dots and applications in photocatalytic energy conversion," *ACS Applied Materials & Interfaces*, vol.7, pp. 8363-8376, 2015.

[26] R. Atchudan, T. N. J. I. Edison, S. Perumal, and Y. R. Lee, "Indian gooseberry-derived tunable fluorescent carbon dots as a promise for in vitro/in vivo multicolor bioimaging and fluorescent ink," *ACS Omega*, vol. 3, pp. 17590-17601, 2018.

[27] D. Carolan, C. Rocks, D. B. Padmanaban, P. Maguire, V. Svrcek, and D. Mariotti, "Environmentally friendly nitrogen-doped carbon quantum dots for next generation solar cells," *Sustainable Energy Fuels*, vol. 1, pp. 1611-1619, 2017.

[28] X. Da, Z. Han, Z. Yang, D. Zhang, R. Hong, C. Tao, H. Lin, and Y. Huang, "Preparation of multicolor carbon dots with high fluorescence quantum yield and application in white LED," *Chemical Physics Letters*, vol. 794, pp. 139497, 2022.

[29] Q. Liu, S. Xu, C. Niu, M. Li, D. He, Z. Lu, L. Ma, N. Na, F. Huang, H. Jiang, and J. Ouyang, "Distinguish cancer cells based on targeting turn-on fluorescence imaging by folate functionalized green emitting carbon dots," *Biosensors and Bioelectronics*, vol. 64, pp. 119-125, 2015.

[30] M. P. Aji, Susanto, P. A. Wiguna, and Sulhadi, "Facile synthesis of luminescent carbon dots from mangosteen peel by pyrolysis method," *Journal of Theoretical and Applied Physics*, vol. 11, pp. 119-126, 2017.

[31] A. Sangjan, S. Boonsith, K. Sansanaphongpricha, T. Thinbanmai, S. Ratchahat, N. Laosiripojana, K. C.W. Wu, H. S. Shin, and C. Sakdaronnarong, "Facile preparation of aqueous-soluble fuorescent polyethylene glycol functionalized carbon dots from palm waste by one-pot hydrothermal carbonization for colon cancer nanotheranostics," *Scientific Reports*, vol. 12, pp. 10550, 2022.

[32] P. Pakorn, S. Sangnuy, and S. Amloy, "Paper-based colorimetric sensor for mercury ion detection using smartphone digital imaging," *Journal of Metals, Materials and Minerals*, vol. 33, no. 2, pp. 81-87, 2023.

[33] D. Li, M. B. Müller, S. Gilje, R. B. Kaner, and G. G. Wallace, "Processable aqueous dispersion of graphene nanosheets," *Nature Nanotechnology*, vol.3, pp. 101-105, 2008.

[34] N. Sharma, I. Sharma, and M. K. Bera, "Microwave-assisted green synthesis of carbon quantum dots derived from Calotropis gigantea as a fluorescent probe for bioimaging," *Journal of Fluorescence*, vol.32, pp. 1039-1049, 2022

[35] H. Lia, S. Hana, B. Lyua, T. Hong, S. Zhia, L. Xuc, F. Xued, L. Saie, J. Yanga, X. Wanga, and B. Heb, "Tunable light emission from carbon dots by controlling surface defects," *Chinese Chemical Letters*, vol. 32, pp. 2887-2892, 2021.